Available online at www.sciencedirect.com

ScienceDirect

Procedia Engineering 199 (2017) 1689–1694

Procedia Engineering

www.elsevier.com/locate/procedia

X International Conference on Structural Dynamics, EURODYN 2017

Including Inerters in Aircraft Landing Gear Shock Strut to Improve the Touch-down Performance

Yuan Li[a], Jason Zheng Jiang[a,*], Pia Sartor[a], Simon A. Neild[a], Huailei Wang[b]

[a] *Faculty of Engineering, University of Bristol, Bristol, UK*

[b] *College of Aerospace Engineering, Nanjing University of Aeronautics and Astronautics, Nanjing, P.R. China*

Abstract

This paper presents the possibility of using inerter-based shock strut in a landing gear to improve aircraft touch-down performance. The inerter is a mechanical element with the property that the applied force is proportional to the relative acceleration between its terminals. The baseline performance of a traditional oleo-pneumatic shock strut is established using a simplified landing gear touch-down model. Several simple layouts and general transfer functions are used to represent the shock struts and time-domain optimisations are carried out to minimise the maximum strut load transmitted to the fuselage during touch-down. The performance benefits of several inerter-based shock strut configurations with the corresponding parameter values have been identified.

Keywords: Shock absorber; touch-down; strut load; passive network; inerter

1. Introduction

It is well known that shock absorber unit plays a significant role in an aircraft landing gear. Complicated design requirements for this unit need to be considered at the design stage of an aircraft. Specifically, under landing touch-down condition, the greatest energy dissipation requirement for the shock absorber is determined, as well as its general performance [1]. For this case, the shock absorber is required to dissipate all the impact energy without causing the aircraft to rebound, with the greatest energy absorption efficiency and the minimum gear load which represents passenger/crew comfort [2]. Nowadays, passive oleo-pneumatic shock absorbers are widely used in aircraft [3].

The inerter is a recently introduced mechanical element, in which the properties are that the applied force is proportional to the relative acceleration between its terminals [5]. With the usage of inerter, a complete analogy between mechanical and electrical systems can be achieved and a much wider range of passive controllers can then be realised by mechanical networks. Recently, the beneficial use of inerters in vibration suppression for a wide range of mechanical structures has been identified, such as in road vehicles [6,7], railway vehicles [8,9], motorcycle steering systems [10,11] and multi-storey buildings [12,13]. References [14,15] considered the application of inerter for suppressing the landing gear shimmy vibration.

* Corresponding author. Tel.: +44 (0)117 95 45612.
E-mail address: z.jiang@bristol.ac.uk

10.1016/j.proeng.2017.09.366

In this paper we investigate the performance advantages of a passive shock strut consisting of linear spring, damper and inerter elements during aircraft touch-down process. The paper is organised as follows. Section II presents a landing gear touch-down model and the dynamics of a conventional oleo-pneumatic shock absorber. Baseline performances are identified and landing touch-down performance criteria are then proposed. In Section III, the optimisation is performed using proposed candidate shock-strut layouts and minimising the maximum shock strut load. Beneficial inerter-based shock-strut configurations are identified. Conclusions are drawn in Section V.

2. Landing gear touch-down model and performance criteria

In this section, a two-degree-of-freedom (2DoF) landing gear model is reviewed, as well as the dynamics of a conventional oleo-pneumatic shock absorber. The model validity was demonstrated via the comparison between the calculated results and drop-test data [16]. Four performance criteria are then proposed.

2.1. Landing gear model and an oleo-pneumatic shock absorber

A 2DoF model shown in Fig. 1(a) is considered here to capture the aircraft touch-down dynamics. Note that this model is presented to capture the first compressive stroke of the shock strut, i.e., from initial contact with the ground to the first time when the relative velocity of the shock strut is slowed to zero. Such process is defined as the touch-down process in this work. As shown in Fig. 1(a), the strut has a rake angle ϕ and the mass of the gear is split into that above the strut and that below it. M_1 represents the total of the upper gear mass and the fuselage mass acting on the gear and M_2 represents the lower gear mass, with the weight W_1 and W_2 respectively. The vertical deflections of the two masses are denoted by z_1 and z_2, respectively, which are zero just prior to contact being made with the ground. The strut stroke s_s measures the relative deflection of the shock strut, i.e. $s_s = z_1 - z_2/\cos\phi$. The free-body diagram of the touch-down model is shown in Fig. 1(b). Apart from the gravity forces, there are also the aerodynamic lifting force L applied to M_1 and the tyre force F_t applied to M_2. The total aircraft weight is assumed to be fully balanced by lifting force during touch-down and linear force-deflection characteristics of the tyre are also assumed, giving

$$L = W_1 + W_2, \quad F_t = k_t z_2, \tag{1}$$

where k_t is the linear tyre vertical stiffness. Balancing the forces acting on the two masses, the equations of motion for this system are written as follows:

$$\frac{W_1}{g}\ddot{z}_1 + F_s cos\phi + L - W_1 = 0, \tag{2}$$

$$\frac{W_2}{g}\ddot{z}_2 - F_s cos\phi + F_t - W_2 = 0, \tag{3}$$

where F_s is the strut force along the strut axis. A descent velocity $V_0 = 8.86$ ft/s is used at the instant the wheels first touch the ground [16]. Note that only this normal impact condition is considered here because the applicability of the model and parameters used in the analysis was investigated in [16] for this condition.

The schematic view of a conventional oleo-pneumatic shock absorber is illustrated in Fig. 1(c). The hydraulic fluid is within the lower chamber of the strut and the pressurised gas in the upper chamber. When the strut is compressed, the fluid is forced through the orifice producing a damping force. Meanwhile, the air is compressed and provides a gas spring force [17]. Then the total strut force can be expressed by

$$F_s = F_h + F_a, \tag{4}$$

where F_h and F_a denote the hydraulic damping force and air spring force, respectively. The expressions of these two forces are given by

$$F_h = A_d|\dot{s}_s|\dot{s}_s, \quad F_a = p_{a_0}A_a(\frac{v_0}{v_0 - A_a s_s})^n, \tag{5}$$

where the parameter definitions of A_d, p_{a_0}, A_a, v_0 and n are illustrated in Table 1. Further details of the shock absorber model can be found in [16].

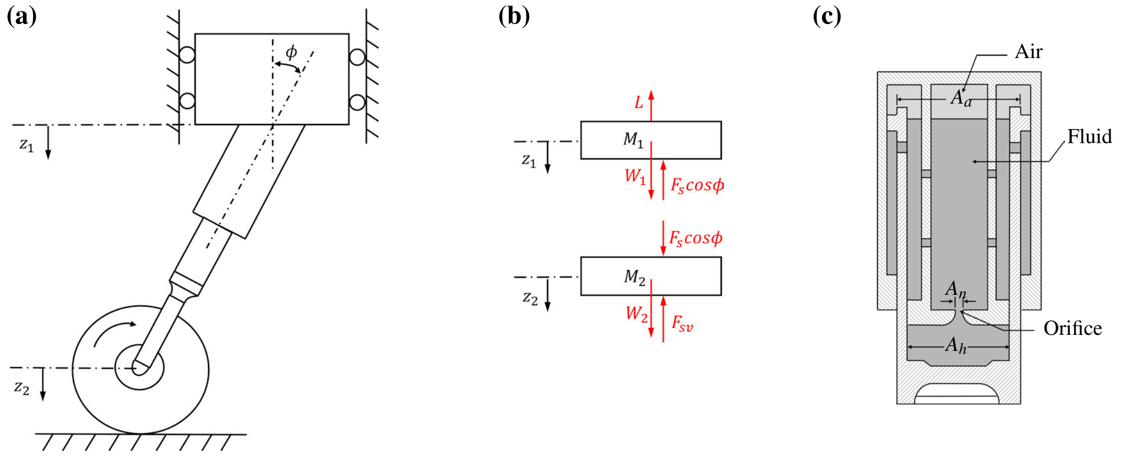

Fig. 1. (a) The dynamic system, (b) the free-body diagram of the model, (c) schematic view of the oleo-pneumatic shock strut (inspired by [16].

The parameter values of the landing gear touch-down model and the conventional shock absorber used in [16] and in this paper are summarised in Table 1. A few values (noted by *) were not given in [16] but have been provided in Table 1 by matching the responses shown in [16].

Table 1. The parameter values used in the analysis

Parameter	Name	Value	Unit
A_a	Pneumatic area	0.05761	ft^2
$A_d{}^*$	Damping factor of oil damping	339.5	$lb_F \cdot s^2/ft^2$
g	Gravitational constant	32.18	ft/s^2
$k_t{}^*$	Vertical tyre stiffness	18500.0	lb_F/ft
n	Polytropic exponent for air-compression process	1.12	-
p_{a_0}	Initial air pressure	6264	lb_F/ft^2
v_0	Initial air volume	0.03545	ft^3
V_0	Descent velocity	8.86	ft/s
W_1	Weight of upper mass	2411	lb_F
W_2	Weight of lower mass	131	lb_F
ϕ^*	Rake angle	12.0	°

2.2. Proposed performance criteria

According to the design requirements for touch-down case, namely, to dissipate all the impact energy with the greatest energy absorption efficiency and minimum gear load, four performance criteria are taken into consideration here. First criterion is the maximum strut load applied to the fuselage, F_{smax}. It is of significance considering passenger discomfort and undesirable structural loading. The maximum strut stroke s_{smax} is regarded as the second criterion. Due to the space limit of a landing gear, a smaller s_{smax} is more preferable. The third criterion is the shock-strut efficiency, η_s, which represents the energy absorption ability of the shock strut. Following [3], η_s is defined as

$$\eta_s = \frac{\int_0^{s_{smax}} F_s ds_s}{s_{smax} F_{smax}}. \tag{6}$$

Moreover, the reduction of kinetic energy during touch-down process is treated as the last performance criterion. Since the same operation condition $V_0 = 8.86$ ft/s is considered for the following discussion, we use the absolute value of the aircraft vertical velocity at the end of touch-down process, $|V_{end}|$, to represent the last criterion, which is given by

$$|V_{end}| = |\dot{z}_1(t_{end})|, \tag{7}$$

where t_{end} marks the end of touch-down, when $\dot{z}_1 - \dot{z}_2 = 0$ for the first time after the wheels touch the ground.

3. Optimisation results

Four candidate shock strut layouts are proposed first in this section. The response of the landing gear with the conventional shock absorber is treated as the baseline for the optimisation. The maximum strut load is used as the objective function while the remaining performance criteria as constraints. The beneficial shock-strut configurations and the corresponding performance improvements are identified from optimisation. In the following discussion, the notation 'L' is used to specify the mechanical network layout and 'C' is for the configurations which represent optimised layouts with the value for each element identified.

3.1. Optimisation procedure and candidate layouts

Using the values in Table 1, the baseline touch-down performance can be calculated that $F_{smaxd} = 6380.3\,\mathrm{lb_F}$, $s_{smaxd} = 0.53$ ft, $\eta_{sd} = 81.5\%$, and $|V_{endd}| = 2.09$ ft/s (the additional subscript 'd' stands for 'default'). In this paper, the maximum strut load F_{smax} will be used as the objective function to be minimised, with the constraint that the remaining three performance criteria must be no worse than that with the default configuration, i.e. $s_{smax} \leq s_{smaxd}$, $\eta_s \geq \eta_{sd}$, $|V_{end}| \leq |V_{endd}|$. For the optimisations performed in the present work, we used the Matlab command `patternsearch` first and then `fminsearch` for fine-tuning of the parameters.

Four candidate shock-strut layouts are proposed here, as shown in Fig. 2. Note that for each layout there will be a spring in parallel, k_s, to make sure that the aircraft can be supported by the landing gear at the rest position. The lower bound for k_s is set to $\overline{k}_s = 4884.2\,\mathrm{lb_F/ft}$ such that the deflection of the gear matches that of the default gear when supporting the aircraft at rest ($s_s = 0.50$ ft for a force of $2464.9\,\mathrm{lb_F}$). Among the four layouts, L1 is the parallel spring-damper layout; L2 includes an inerter in parallel with L1; L3 is the layout of a series inerter-damper arrangement in parallel with k_s; LY represents a general layout with k_s in parallel. Optimisations will be carried out over these four layouts and for each layout, it will be conducted for the case where $k_s = \overline{k}_s$ and for $k_s > \overline{k}_s$.

When designing mechanical vibration absorbers, one of the crucial demands is to minimise the layout complexity due to space and weight limit. The potential of layouts with the lowest complexity can be investigated using L1–L3 while LY allows for a more complex mechanical structure to be considered. In this paper, a general positive-real frequency function $Y(s)$ is considered to represent layout LY, giving

$$\widetilde{F_s}(s) = (Y(s) + \frac{k_s}{s})\widetilde{\dot{s}_s}(s), \tag{8}$$

where s is the Laplace variable, $\widetilde{F_s}(s)$ and $\widetilde{\dot{s}_s}(s)$ are the force and the relative velocity of the strut in the Laplace domain, respectively. $Y(s)$ can be realised by a network consisting of springs, dampers and inerters using the network synthesis method [18]. In order to reduce the complexity of LY but still covering a reasonable range of possibilities, $Y(s)$ is set to be a biquadratic function, in which the numerator and denominator are second-order functions of s,

$$Y(s) = \frac{As^2 + Bs + C}{Ds^2 + Es + F}, \tag{9}$$

where the parameter values $(A, B, \cdots, F)$ are all non-negative and are chosen via optimisation. When considering $k_s = \overline{k}_s$, the constraint $F > 0$ is considered to ensure that $Y(s)$ does not require an additional parallel spring to supplement k_s. Based on the optimal values of A, B, $\cdots$, F, the corresponding network can be identified. Then we would apply a simplification procedure to investigate whether a simpler layout may be used. The first step is to check whether the performance deteriorates significantly when the least significant element(s) is/are removed, for example, the elements whose values are small (when in parallel) or large (when in series) compared with the remaining ones. After that, new optimisation is performed over the simplified network layout and to identify the optimal element values. Similar procedures have been successfully demonstrated in [13,15].

3.2. Identified beneficial configurations

The optimisation results are summarised in Table 2. Note that the subscript v is used to specify the case when k_s is allowed to be variable (the $k_s > \overline{k}_s$ case). No improvement over the default system was identified for the case where

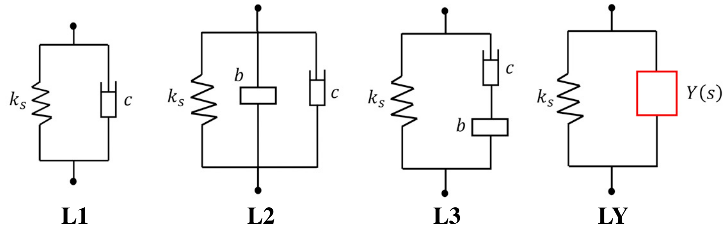

Fig. 2. Four candidate shock-strut layouts.

layouts L1–L3 and $k_s = \bar{k}_s$ are considered. Hence Table 2 only summarised the results for layouts L1–L3 with $k_s > \bar{k}_s$. Comparing with the baseline system, the configuration C1$_v$ can provide a 12.5% reduction in F_{smax}, and the optimum configurations C2$_v$ and C3$_v$ decrease F_{smax} by 21.4% and 21.6%, respectively. The advantages of including an inerter can be seen by comparing the performance obtained with C2$_v$ and C3$_v$ to that of the non-inerter C1$_v$. Reductions in F_{smax} by 10.3% and 10.4% respectively are obtained, which can be attributed to the inclusion of an inerter. Besides, it should be noted that in C3$_v$ a much higher damping value is required, which is likely to be impractical.

Table 2. Optimisation results using layouts L1–LY

Configurations	F_{smax} (lb$_F$)	Improvement (%)	Layouts	Optimum parameter values (lb$_F$/ft, lb$_F \cdot$ s/ft, lb$_m$)
Default	6380.3	-	-	-
C1$_v$	5581.0	12.5	L1	$k_s = 9043.9, c = 535.2$
C2$_v$	5014.5	21.4	L2	$k_s = 16163, c = 60.21, b = 18.1$
C3$_v$	5003.9	21.6	L3	$k_s = 16927, c = 12171, b = 19.2$
CY	5004.9	21.6	L4	$k_s = 4884.2, c_1 = 3817.1, c_2 = 404.9, b = 9.4, k_1 = 6874.1$
CY$_v$	4976.5	22.0	L5	$k_s = 8049.2, c_1 = 8492.6, c_2 = 9089.1, b = 20.6, k_1 = 9031.3$

In contrast to the simpler layouts L1–L3, when $k_s = \bar{k}_s$, a 21.6% reduction in F_{smax} can be obtained by CY. Using relevant network synthesis theory, the network realisation is identified and shown in Fig. 3(a) as layout L4. In this layout, an inerter is in parallel with the supporting stiffness, as well as a combination of two dampers and an internal spring. Note that layout L4 can be reduced to L2 if c_1 in L4 is set to infinity. Configuration CY$_v$ provides the maximum improvement in F_{smax}, with up to 22.0% reduction. The resulting mechanical network, labelled L5, is illustrated in Fig. 3(a). Note that both layouts L4 and L5 consist of five mechanical elements but in different arrangements. Further optimisations over L4 and L5 in which the inerter is removed are carried out. Based on the results and the simplification procedure, it can be found that both the optimal solutions are similar with the C1$_v$ configuration. This suggests the performance improvements obtained by CY (layout L4) and CY$_\eta$ (layout L5) require the inclusion of the inerter.

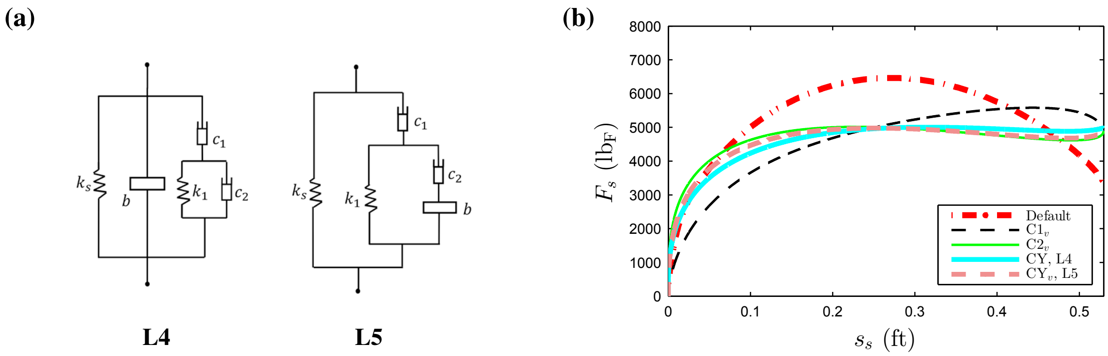

Fig. 3. (a) Layouts L4 and L5, which correspond to configurations CY and CY$_v$, respectively, (b) the improved load-stroke curves.

Hence, considering the performance improvements and practical parameter values, we treat $C2_v$, CY and CY_v as the optimum configurations for the F_{smax} optimisation. The load-stroke curves provided by the optimum struts, as well as the default and $C1_v$ configuration, are compared in Fig. 3(b). In addition, since for a normal landing the aircraft descent velocity may be lower than 8.86 ft/s, a further analysis for checking landing performances when considering a wide range of descent velocities (3-8.86 ft/s) and assuming the model is always applicable is carried out. It can be found that all the inerter-equipped landing gears will be beneficial than the default system for the full range of velocities considered.

4. Conclusions

This paper has investigated the potential benefits of inerter-integrated shock struts for minimising the maximum strut load applied to the fuselage during aircraft touch-down process. Based on a 2DoF model with the conventional oleo-pneumatic shock absorber, the baseline touch-down performances are obtained. With the restriction that the optimum shock struts obtain the touch-down performance no worse than the baseline system, the optimisations have been carried out using four candidate shock strut layouts. With a five-element configuration and an increased static spring, up to 22.0% reduction on the maximum strut load is obtained comparing with the default system. The benefits of including an inerter in the layout are also evidenced.

Acknowledgments

The authors would like to acknowledge the support of the EPSRC and the China Scholarship Council (CSC): Simon Neild is supported by an EPSRC fellowship EP/K005375/1 and Yuan Li supported by a CSC studentship.

References

[1] S.F.N. Jenkins, Landing gear design and development, Proceedings of the Institution of Mechanical Engineers, Part G: Journal of Aerospace Engineering, 203.1 (1989) 67–73.
[2] H.P.Y. Hitch, Aircraft ground dynamics, Vehicle System Dynamics, 10.4-5 (1981) 319–332.
[3] N.S. Currey, Aircraft landing gear design: principles and practices, AIAA Education, New York, 1988.
[4] X. Wang, U. Carl, Fuzzy control of aircraft semi-active landing gear system, Proceeding of the 37th AIAA Aerospace Sciences Meeting and Exhibit, 1999.
[5] M.C. Smith, Synthesis of mechanical networks: the Inerter, IEEE Transactions on Automatic Control, 47.10(2002) 1648–1662.
[6] Y. Shen, L. Chen, X. Yang, D. Shi, J. Yang, Improved design of dynamic vibration absorber by using the inerter and its application in vehicle suspension. Journal of Sound and Vibration, 361(2016) 148–158.
[7] F. Scheibe, M.C. Smith, Analytical solutions for optimal ride comfort and tyre grip for passive vehicle suspensions, Vehicle System Dynamics, 47.10(2009) 1229–1252.
[8] J.Z. Jiang, A.Z. Matamoros-Sanchez, R.M. Goodall, M.C. Smith, Passive suspensions incorporating inerters for railway vehicles, Vehicle System Dynamics, 50.sup1(2012) 263–276.
[9] J.Z. Jiang, A.Z. Matamoros-Sanchez, A. Zolotas, R.M. Goodall, M.C. Smith, Passive suspensions for ride quality improvement of two-axle railway vehicles, Proceedings of the Institution of Mechanical Engineers, Part F: Journal of Rail and Rapid Transit, 2013.
[10] J.Z. Jiang, M.C. Smith, N.E. Houghton, Experimental testing and modelling of a mechanical steering compensator, The 3rd Int. Symp. Communications, Control Signal Processing (ISCCSP), 2007, pp. 249–254.
[11] D. Limebeer, R. Sharp, S. Evangelou, M. Smith, An H_∞ loop-shaping approach to steering control for high-performance motorcycles, Lecture notes in Control and Information Sciences, Springer, New York, 329(2006) 257–275.
[12] I.F. Lazar, S.A., Neild, D.J. Wagg, Using an inerter-based device for structural vibration suppression, Earthquake Engineering & Structural Dynamics, Wiley Online Library, 43.8(2014) 1129–1147.
[13] S.Y. Zhang, J.Z. Jiang, S.A. Neild, Optimal configurations for a linear vibration suppression device in a multi-storey building, Structural Control and Health Monitoring, 2016.
[14] D. Xin, L. Yuance, M.Z. Chen, Application of inerter to aircraft landing gear suspension, 34th Chinese Control Conference, IEEE, 2015, pp. 2066–2071.
[15] Y. Li, Z. Jiang, S.A. Neild, Inerter-based configurations for main landing gear shimmy suppression, Journal of Aircraft, 2016. DOI: 10.2514/1.C033964.
[16] B. Milwitzky, F.E. Cook, Analysis of landing gear behavior, NACA Report 1154, 1953.
[17] D. Yadav, R.P. Ramamoorthy, Nonlinear landing gear behavior at touchdown, ASME Journal of Dynamic Systems, Measurement, and Control, 113.4(1991) 677–683.
[18] R. Bott, R.J. Duffin, Impedance synthesis without use of transformers, Journal of Applied Physics, 20.8(1949) 816–816.